AGU ADVANCING EARTH AND SPACE SCIENCES

Water Resources Research

RESEARCH ARTICLE
10.1029/2024WR039346

Special Collection:
Advances in large-scale hydrological modeling and prediction under global change

Groundwater Storage Changes Using GRACE and ESA CCI Soil Moisture Products in Southern Victoria, Australia

Taejun Park[1], Ki-Weon Seo[1], Dongryeol Ryu[2], Jae-Seung Kim[2,3], Daeha Lee[1], Jianli Chen[4,5,6], and Clark R. Wilson[7,8]

[1]Department of Earth Science Education, Seoul National University, Seoul, Republic of Korea, [2]Department of Infrastructure Engineering, The University of Melbourne, Melbourne, VIC, Australia, [3]Center for Educational Research, Seoul National University, Seoul, Republic of Korea, [4]Department of Land Surveying and Geo-Informatics, The Hong Kong Polytechnic University, Hong Kong, China, [5]Research Institute for Land and Space, The Hong Kong Polytechnic University, Hong Kong, China, [6]The Hong Kong Polytechnic University Shenzhen Research Institute, Shenzhen, China, [7]Center for Space Research, University of Texas at Austin, Austin, TX, USA, [8]Department of Earth and Planetary Sciences, Jackson School of Geosciences, University of Texas at Austin, Austin, TX, USA

Abstract Groundwater depletion, driven by climate change and increasing extraction for irrigation, has increased the need for accurate monitoring. Traditional methods, such as in situ water table observations and pumping tests, are valuable for assessing groundwater availability and aquifer characteristics but are limited in capturing basin-scale variations. The Gravity Recovery and Climate Experiment (GRACE) enables estimation of basin-scale groundwater changes, though its observations also include surface water and soil moisture (SM) in the vadose zone. Therefore, additional data on non-groundwater components are needed to isolate groundwater variations. In this study, we use the profile SM content for the top 0–120 cm of soil as an estimate of vadose zone SM, derived using an exponential filtering technique applied to European Space Agency's Climate Change Initiative for Soil Moisture (ESA CCI SM) and in situ data. This approach addresses limitations of conventional models, such as their inability to represent non-natural or lateral water redistribution. Groundwater storage (GWS) changes in southern Victoria, Australia were estimated by subtracting the filtered SM from GRACE data and validated against in situ groundwater level observations for both unconfined and confined aquifers. The ESA CCI SM-based estimates showed clear improvements in capturing seasonal and interannual variability of in situ GWS compared to conventional model-based estimates. The proposed approach is potentially applicable to GWS estimation at continental scales.

Plain Language Summary Conventional groundwater studies rely on measurements of the water table in sparsely distributed bore holes, and are suitable for small spatial scales. The Gravity Recovery and Climate Experiment (GRACE) mission measures total terrestrial water storage over large spatial scales via changes in gravity. Thus it is necessary to remove surface water and soil moisture (SM) components to separate the groundwater signal in GRACE observations. Past studies have estimated surface water and SM variations using numerical models, but here we use satellite SM observations from microwave sensors from the European Space Agency's Climate Change Initiative. We estimate groundwater changes for the southern region of Victoria, Australia, and validate them with in situ borehole level change data. Our estimates showed better agreement with in situ observations than those from conventional model-based approaches, indicating the potential of this method for continental-scale groundwater storage studies.

Key Points:

- Groundwater storage changes in southern Victoria, Australia are estimated using multiple remote sensing data, with greater accuracy than traditional model-driven methods
- The estimated groundwater storage changes are consistent with in situ observations from both unconfined and confined aquifers at the basin scale

Supporting Information:

Supporting Information may be found in the online version of this article.

Correspondence to:

K.-W. Seo,
seokiweon@snu.ac.kr

Citation:

Park, T., Seo, K.-W., Ryu, D., Kim, J.-S., Lee, D., Chen, J., & Wilson, C. R. (2025). Groundwater storage changes using GRACE and ESA CCI soil moisture products in southern Victoria, Australia. *Water Resources Research*, *61*, e2024WR039346. https://doi.org/10.1029/2024WR039346

Received 1 NOV 2024
Accepted 2 OCT 2025

1. Introduction

Except for glaciers and ice sheets, approximately 96% of Earth's freshwater resources lie beneath the surface as groundwater. Groundwater supplies nearly 50% of the world's drinking water and 43% of irrigation water in agriculture (Smith et al., 2016). There is greater reliance on groundwater, as well, in mid-latitude arid and semi-arid regions, where large groundwater depletion rates are found in almost every major aquifer (Frappart & Ramillien, 2018). Moreover, 30% of the world's regional aquifers have shown accelerated groundwater level decline over the last 40 years (Jasechko et al., 2024). Examples include groundwater depletion in North India (Dangar et al., 2021), North China Plain (Feng et al., 2018), the High Plains aquifer and the Central Valley of California in the United States (Konikow, 2015) and Iran (Ashraf et al., 2021). About 1.7 billion people live in

areas where groundwater depletion is a problem (Gleeson et al., 2012). Accurate assessment and monitoring of groundwater change are essential to assist in planning sustainable water resource management.

Traditionally, groundwater is monitored by in situ measurement of groundwater levels in combination with aquifer property assessment through drilling and pumping tests. However, these methods are limited to areas near the measurement point and may not adequately represent larger areas. A dense monitoring network needed for an unbiased regional view is rarely available. Satellite gravity observations from the Gravity Recovery and Climate Experiment (GRACE) mission provides useful and accurate large-scale groundwater storage change information. The GRACE mission was launched in March 2002 as a joint effort of the National Aeronautics and Space Administration (NASA) and the German Aerospace Center (DLR). Precise (micrometer-level) measurement of changing distance between a satellite pair in polar orbit is used to calculate gravitational force changes beneath the satellites (Tapley et al., 2019). GRACE provided monthly solution for changes in Earth's gravity field until the mission ended in October 2017.

GRACE data have been used in terrestrial water storage (TWS) research to measure the total of surface water (river, lake, snow, and other reservoirs on the surface) and subsurface water (soil water and groundwater). Separating surface water (e.g., lakes and rivers) from TWS is relatively straightforward because it can be observed directly. However, isolating soil moisture (SM) from TWS is more difficult. There have been considerable efforts to establish global SM monitoring networks, such as the International Soil Moisture Network (ISMN, https://ismn.earth/en/), but existing in situ SM monitoring still provides limited spatial and temporal coverage. As a result, SM estimated by land surface models (LSM) has been employed to separate groundwater storage change from GRACE TWS observations. As examples, GRACE TWS and LSM SM were used to estimate aquifer storage changes in the High Plains aquifer (Strassberg et al., 2007), the Central Valley in California (Famiglietti et al., 2011), the Canning basin of Australia (Munier et al., 2012), the Great Artesian Basin of Australia (Castellazzi et al., 2024), and in Northern India (Rodell et al., 2009). However, most LSMs are limited in their ability to accurately estimate SM in the vadose zone, primarily because they do not clearly distinguish it from the saturated zone. Also, a one-dimensional column structure of typical LSMs neglects horizontal flow of both runoff (without explicitly accounting for routing and re-infiltration) and soil water, leading to potential errors in GWS estimation (Condon et al., 2021). Moreover, the cited GRACE studies have ignored spatial leakage in GRACE TWS estimates. Spatial leakage of GRACE signals among basins and from land to oceans may bias TWS estimates resulting in biased groundwater estimates. The leakage problem is particularly important for small basins and for those adjacent to the oceans.

In this study, we estimate groundwater storage variations in the southern region of Victoria, Australia, using GRACE data. This region has been affected by a severe "Millennium Drought," from the 1997 to 2009. The Millennium Drought substantially influenced subsurface water storage (Fowler et al., 2020; Weligamage et al., 2023) and runoff, with 37% of watersheds in the region not recovering 7 years after the drought (Peterson et al., 2021). Understanding groundwater depletion during the drought and recovery afterward will lead to understanding of changes in runoff, evapotranspiration and long-term effects on the terrestrial water cycle. Previously, Chen et al. (2016) estimated groundwater variations in this region using GRACE TWS and compared them with in situ observations. As in similar studies, LSM SM estimates of SM variations were employed. They used the forward modeling method to correct for spatial leakage, which is effective in suppressing land to ocean leakage but does not reduce inter-basin leakage.

To address potential limitations associated with using LSM-derived SM for GWS estimation, we separate SM content from GRACE TWS using the European Space Agency-Climate Change Initiative soil moisture (ESA CCI SM) product, which combines data from various microwave satellites. ESA CCI SM for the top soil layer (a few centimeters) is extended to estimate SM of the entire root zone using an exponential filtering technique. Water beyond the root zone is assumed to drain to the aquifer below. The exponential filtering technique has been employed extensively to estimate root zone SM content using the top soil layer with in situ SM measurements as references (Albergel et al., 2008). In this study, exponential filtering applied to the ESA CCI SM is calibrated using in situ SM measurements to estimate profile SM content. It is assumed that by using the profile SM derived from microwave surface SM, we can improve the profile SM estimate over the conventional estimates from LSM, which present limited representation of non-natural or horizontal redistribution of water. In addition, we used leakage-corrected TWS data derived from constrained linear deconvolution (CLD) (Kim et al., 2024). CLD provides TWS with higher spatial resolution by suppressing spatial leakage, considering both a priori LSM TWS

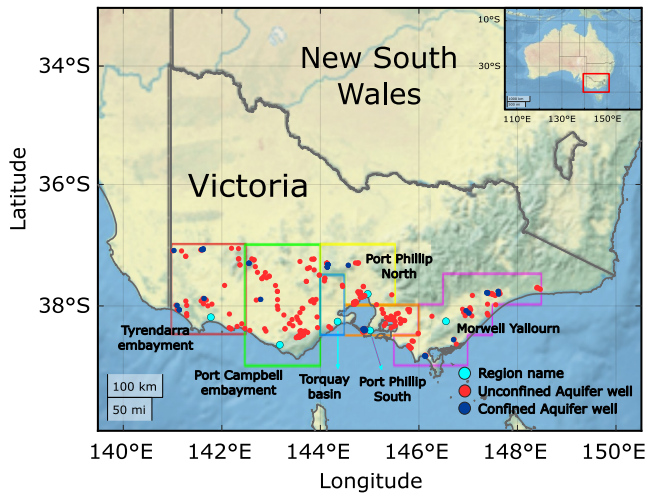

Figure 1. Distribution of unconfined and confined aquifer wells within six sub-basins in southern Victoria.

and GRACE TWS data. Addressing coastline and inter-basin leakage is important in this case because the southern region of Victoria is bordered by the coastline to the south and the Murray-Darling basin to the north.

Lastly, previous studies presented limited validation of GRACE-derived GWS due to sparse ground data with simplified assumptions: consideration of unconfined aquifers only, an arbitrary choice of specific yield, or uniform specific yield assumed across the entire basin. In this study, we propose a method to estimate aquifer parameters using GRACE-derived GWS in conjunction with dense in situ groundwater level data. This approach enables verification of the method and robust validation of the resulting GWS estimates.

2. Data and Method

2.1. Terrestrial Water Storage (TWS)

We used TWS estimates from GRACE observations after removing spatial leakage between land and oceans and among basins following the CLD approach of Kim et al. (2024). To suppress leakage and enhance spatial resolution of TWS data to 0.5° by 0.5°, GRACE observations are combined with European Centre for Medium-Range Weather Forecasts (ECMWF) Reanalysis version 5 (ERA5) model data in the CLD. In this study, we used a total of 157 monthly data sets from May 2002 to May 2015 considering the common period of sufficient data availability with groundwater level in situ data. We calculated the spatial average of TWS over six sub-basins where groundwater information is available (Figure 1).

2.2. Groundwater In Situ Data

We utilized in situ groundwater level time series data (1 January 2000–31 December 2020) provided by the Bureau of Meteorology (BoM, http://www.bom.gov.au). Most wells are sampled at 3-month intervals. To select groundwater data most suitable for our analysis, we first excluded stations with a small number of samples (fewer than 20). Then, we removed evident outliers with departures exceeding 20 m from the station mean. Finally, groundwater level data with abrupt shifts or abnormal variations were excluded using visual inspection. These were likely affected by a pumping test or other local factors. This left 430 of the original 549 wells (bore holes), south of 37°S within Victoria (Figure 1). There are fewer bore holes in the east due to increasing elevation of the highland mountains. Data were aggregated to monthly values (3-month intervals) to match GRACE sample times, to obtain 53 months of data, from May 2002 to May 2015 (Figure S1 in Supporting Information S1).

The 430 wells were separate into those for confined and unconfined aquifers. Confined aquifers depths are typically deeper than for unconfined aquifers. In southern Victoria, there are three main basins, the Otway, Central coast, and Gippsland basins. The vertical structure of aquifers and aquitards has been classified by (GHD, 2012) at sub-basin scales, with average thicknesses at (https://www.water.vic.gov.au/). These estimates were used to set average depths to the top of the uppermost aquitards (Table 1). We then compared the bottom depths of the selected 430 wells to the aquitard depths shown in Table 1 to classify the aquifers as confined and unconfined. Bottom depths of unconfined aquifers are shallower than aquitards, while those of confined aquifers are deeper.

Table 1
Depth to the Top of Uppermost Aquitard of Each Sub-Basin

Name of the sub-basins	Depth to the top of uppermost aquitard
Tyrendarra embayment	178 m
Port Campbell embayment	144 m
Torquay basin	91 m
Port Phillip basin (North)	80 m
Port Phillip basin (South)	33 m
Morwell Yallourn	35 m

We converted the selected monthly groundwater level data to monthly anomalies for comparison with GRACE data. The observation period varies for each well, so conversion to monthly anomalies requires care to avoid possible biases using mean values determined from different periods. To address this, we first selected wells with near-complete data coverage throughout the period from May 2002 to May 2015, with less than one year of consecutive missing data. From these we calculated average variations within each 0.5° grid interval near the selected wells, and then used these to correct remaining well data with shorter observation periods and/or missing data. Finally, other wells were adjusted to align with the reference wells, assuming mean values during their common observation period are identical at each

grid interval. The same process was applied for both confined and unconfined aquifers.

To distinguish between unconfined and confined aquifer wells accurately, we applied an additional filtering process. For confined aquifer level changes, we excluded wells with a mean seasonal amplitude larger than that of unconfined wells, based on the general understanding that confined aquifers exhibit smaller annual fluctuations. This filtering process was performed separately for each of the six sub-basins. As a result, we retained 40 confined aquifer wells and 284 unconfined wells for the analysis.

2.3. Surface Water

We used the Water Global Assessment and Prognosis (WaterGAP) v2.2d model data (Schmied et al. (2021)). WaterGAP provides monthly global estimates for all continental areas on a 0.5° grid since 1996, for all surface water components, including canopy, snow, lake, wetland, and river storage. Among surface water components, we used the sum of canopy, river, and lake storage from May 2002 to May 2015. Other contributors were either zero or negligible in southern Victoria. We spatially averaged WaterGAP estimates to match grids used for groundwater data analysis in Figure 1. The spatially-average WaterGAP data were converted to monthly anomalies by subtracting mean values for the study period. WaterGAP anomalies were used to correct GRACE TWS for surface water variations, so uncertainties in WaterGAP estimates will contribute to uncertainty in groundwater estimates which are the focus of this study.

2.4. Soil Moisture

The ESA CCI SM v8.1 combined product is a blend of scatterometer and radiometer observations, providing daily surface SM at a spatial resolution of 0.25° globally from 1 November 1978 to 31 December 2022 (Dorigo et al., 2023). We averaged daily solutions to monthly values. CCI SM provides volumetric moisture content (m^3/m^3) for about the top 2 cm layer. To estimate the moisture content in the entire root zone, we used an EF method widely used to estimate root zone SM content from surface SM content. It was originally proposed by Wagner et al. (1999) and refined in the recursive form by Stroud (1999) and Albergel et al. (2008). The original EF approach assumes a single soil layer and does not account for depth-dependent soil properties. To address this limitation, Pasik et al. (2023) modified the EF by employing a multi-layer root zone model, where SM in each sub-surface layer is estimated independently from the surface SM using the EF. In our study, we further improved this multi-layer EF method by implementing the EF sequentially across adjacent layers to ensure more gradual propagation of SM response between them. The multi-layer EF used in this study is:

$$\mathrm{SWI}_t^i = \mathrm{SWI}_{t-1}^i + K_t^i\left(\mathrm{SWI}_t^{i-1} - \mathrm{SWI}_{t-1}^i\right), \tag{1}$$

$$K_t^i = \frac{K_{t-1}^i}{K_{t-1}^i + e^{-\Delta t/T^i}} \tag{2}$$

where i is soil layer index ($i = 1,\ldots,n$) that increases from the top ($i = 1$) to the bottom layer ($i = n$). SWI_t^0 is the remotely sensed surface SM. The assumption in the above equations is that water flux between two adjacent layers is proportional to the difference in moisture between the layers. K_t is a time-varying gain ranging between 0 and 1, Δt the sampling interval (typically 1 day), and T a constant parameter for smoothing. Depending on SM data availability, Δt can exceed 1 day at some grid points, with a maximum of 7 days in our study.

SWI_t^i $\left(\mathrm{m}^3/\mathrm{m}^3\right)$ estimated via Equations 1 and 2 needs to be rescaled for root zone soil water content (SWC_t^i) using additional information about the minimum ($\mathrm{SWC}_{\mathrm{min}}^i$) and maximum ($\mathrm{SWC}_{\mathrm{max}}^i$) values of SWC^i as:

$$\mathrm{SWC}_t^i = \frac{\mathrm{SWI}_t^i - \mathrm{SWI}_{\mathrm{min}}^i}{\mathrm{SWI}_{\mathrm{max}}^i - \mathrm{SWI}_{\mathrm{min}}^i} \times \left(\mathrm{SWC}_{\mathrm{max}}^i - \mathrm{SWC}_{\mathrm{min}}^i\right) + \mathrm{SWC}_{\mathrm{min}}^i \tag{3}$$

where $\mathrm{SWI}_{\mathrm{max}}^i$ and $\mathrm{SWI}_{\mathrm{min}}^i$ are maximum and minimum values of SWI^i, respectively.

Three parameters (T^i, $\mathrm{SWC}_{\mathrm{min}}^i$ and $\mathrm{SWC}_{\mathrm{max}}^i$) required to convert from SWI_t^i to SWC_t^i were estimated by minimizing the difference between SWC_t^i and in situ soil water content, $\mathrm{SWC}_t^{i,\mathrm{in-situ}}$ $\left(\mathrm{m}^3/\mathrm{m}^3\right)$, obtained from root

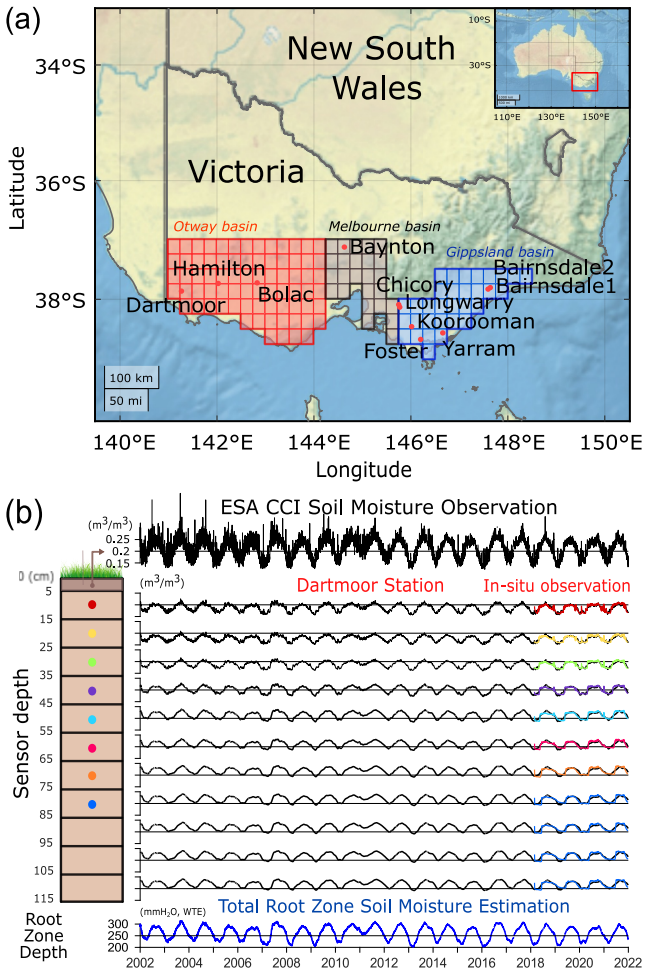

Figure 2. (a) Soil moisture (SM) in situ monitoring stations in southern Victoria. Grids are divided into three basins based on the GHD's study (GHD, 2012). (b) Schematic illustration of the SM measuring sensors at Dartmoor station.

zone SM stations across the study region (Figure 2a), operated by Agriculture Victoria (https://extensionaus.com.au/soilmoisturemonitoring/). Of the 15 stations originally available, 3 with less than one year of data and 1 showing highly irregular vertical profiles were excluded from the analysis. The remaining 11 in situ data, available daily at 10 cm depth intervals, were used for EF calibration at each depth. For Hamilton and Bolac stations, where the first depth layer was at 30 cm, calibration began at 30 cm and continued in 10 cm increments. in situ SM observations from sensors are assumed to represent the soil layer corresponding to the depth of each sensor.

In situ soil water content, $SWC_t^{i,\text{in-situ}}$, is estimated based on in situ sensor observational data $\left(OBS_t^i\ (m^3/m^3)\right)$ via:

$$SWC_t^{i,\text{in-situ}} = OBS_t^i \cdot PAW^i + PWP^i \quad (4)$$

in which PAW^i is plant available water and PWP^i is permanent wilting point, both of which are constant values defined by the soil texture of each soil layer. PAW represents the amount of water required for plant growth which ranges between 0 and 1. When OBS_t^i is zero, $SWC_t^{i,\text{in-situ}}$ becomes PWP^i, the amount of SM when plants start to wilt, and $OBS_t^i = 1$ means SM content has reached the field capacity of soil. The in situ station provides information on the region's investigated soil type along with PAW and PWP values.

Figure 2b shows SM estimates derived using the EF alongside in situ SM observations (m^3/m^3) at the Dartmoor station. The in situ SM sensors at the station are installed at 10 cm depth intervals, ranging from depths of 10–80 cm. The root zone depth in the Dartmoor station area is approximately 120 cm, as reported by Schenk and Jackson (2009). Soil layers without sensors (at depths of 90, 100, 110 cm) in the root zone are assumed to have the same value as the sensor depth of 80 cm. This assumption stems from the observation that variations in SM at greater depths are comparatively smaller than those at shallower depths (Tromp-van Meerveld & McDonnell, 2006). The black line at the top represents daily ESA CCI SM (SWI_t^0) and the shorter colored lines ($SWC_t^{i,\text{in-situ}}$) at sensor depths indicate in situ observations. Parameters of T^i, SWC_{min}^i and SWC_{max}^i were estimated during the common period of each in situ SM (color lines) and ESA CCI SM (black line at the top). The three parameters were used to estimate the root zone SM (SWC_t^i) via EF from 1 January 2003 to 31 December 2021 (black lines at sensor depths). Total root zone SM estimation (blue line at the bottom of Figure 2b) is the sum of actual water storage variation (kg/m^2) of each layer, derived via multiplying each SWC_t by water density and layer thickness (10 cm).

We applied the same EF approach to 10 more stations and acquired EF parameter sets for each location (T^i, SWC_{min}^i and SWC_{max}^i values for each sensor depths). The estimated EF parameters and SM for all 11 stations are provided in Supporting Information S1 (Table S1 and Figure S2). The EF approach was applied to all grid cells of the ESA CCI SM to compute root zone water storage. We categorized all gridded areas into three basins based on hydrogeological characteristics defined in the GHD survey (GHD, 2012). These basins are visually distinguished by different colors in Figure 2a. For each basin, we applied a uniform EF parameter set, derived as the average of EF parameters calibrated at the in situ stations within that basin, along with the average root zone depth obtained from Schenk and Jackson (2009). The root zone depths applied to each of the three basins (Otway, Melbourne, and Gippsland basin) are 115 cm, 125 cm, and 125 cm, respectively. These values represent the average root zone depths derived from the one grid interval data set provided by Schenk and Jackson for the regions corresponding to the three basins (118.1 cm, 128.0 cm, and 125.1 cm, respectively).

To evaluate the robustness and accuracy of our method, we estimated the SM profiles at the Dartmoor and Chicory station locations using the EF approach and compared them with ground truth observations. The EF-

based estimates showed superior performance compared to ERA5 (Muñoz Sabater, 2019) and Global Land Data Assimilation System (GLDAS) SM (Beaudoing & Rodell, 2020) products. Detailed results and explanations are provided in Supporting Information S1 (Figure S3).

2.5. Groundwater Level and Storage Change

Groundwater storage change (ΔGWS) can be estimated from GRACE TWS change (ΔTWS), SM change (ΔSM), and surface water change (ΔSW) data:

$$\Delta\mathrm{GWS} = \Delta\mathrm{TWS} - \Delta\mathrm{SW} - \Delta\mathrm{SM}. \tag{5}$$

ΔSW and ΔSM were obtained from WaterGAP and ESA CCI via the EF, respectively, as noted above. ΔGWS can also be estimated using groundwater level data (i.e., hydraulic head, Δh) in confined and unconfined aquifers, and their respective capacity to produce water for a given Δh, that is, specific storage (S_s) for confined and specific yield (S_y) for unconfined aquifers. Specific storage (S_s) is defined as "the volume of water that is released from or taken into storage per unit surface area of a confined aquifer or a confined aquifer layer per unit change in hydraulic head" (Batu, 1998). Unlike specific yield (S_y), which is dimensionless, specific storage depends on the depth (b) of a confined aquifer. In fact, many aquifer systems are multi-layered, including both unconfined and confined zones. For a composite aquifer system, total volume of water (ΔV) released or extracted can be represented as the sum of unconfined ($\Delta V_1 = S_y \cdot \Delta h_1$) and confined ($\Delta V_2 = S_s b \cdot \Delta h_2$) aquifers:

$$\Delta V = S_y \cdot \Delta h_1 + S_s b \cdot \Delta h_2. \tag{6}$$

Multiplying water density (ρ) by Equation 6, it becomes groundwater storage change (ΔGWS):

$$\Delta\mathrm{GWS} = S_y \cdot \rho \cdot \Delta h_1 + S_s b \cdot \rho \cdot \Delta h_2. \tag{7}$$

S_y and $S_s b$ were estimated using generalized least squares based on the estimated ΔGWS and in situ groundwater changes, Δh_1 and Δh_2, as described in Equation 8. The estimated S_y and $S_s b$ values can be considered representative aquifer parameters for the study area. The plausibility of these values further supports the validity of the results.

$$m = \left[G^T G\right]^{-1} G^T d \tag{8}$$

Here, m consists of two elements, S_y and $S_s b$. G is a kernel matrix including Δh_1 and Δh_2 at each row. d is a row matrix of $\Delta\mathrm{GWS}/\rho$. Uncertainties in estimated S_y and $S_s b$ can be obtained from the covariance matrix, C_m (Menke, 2012):

$$\sigma_d^2 \approx \frac{1}{N - M} e^T e \tag{9}$$

$$C_m = \sigma_d^2 \left[G^T G\right]^{-1} \tag{10}$$

where e is prediction error, defined as $e = d - Gm$. N (=53) are the number of observations and M (=2) the number of model parameters.

3. Results and Discussions

3.1. Mean Groundwater Level Variations

Figure 3 shows mean in situ groundwater level variations of unconfined (red) and confined aquifers (blue) in southern Victoria. Unconfined aquifers show evident seasonal and inter-annual variations. Annual level fluctuations in confined aquifers tend to be smaller than unconfined. Unconfined aquifers are directly influenced by atmospheric pressure and precipitation, whereas confined aquifers, under high pressure from overlying layers, are

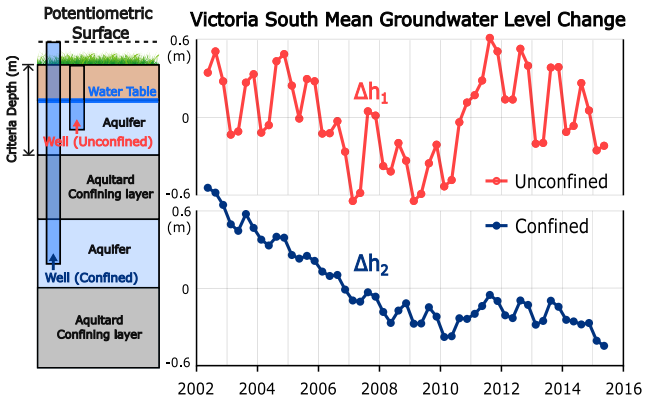

Figure 3. Schematic illustration of unconfined and confined aquifer groundwater level changes in southern Victoria, respectively.

less susceptible to these external influences. Specific examples for individual wells can be found in Figure S4 in Supporting Information S1.

For 2002–2010, part of "The Millennium Drought", mean groundwater levels for both confined and unconfined aquifers show a decline, followed by recovery between 2010 and 2011 with increased precipitation caused by a strong La Niña (http://www.bom.gov.au/climate/history/enso/). After 2011, both confined and unconfined experienced a gradual decline, likely due to decreased precipitation and a second drought (http://www.bom.gov.au/climate/drought/knowledge-centre/previous-droughts.shtml). More increasing and decreasing trends are seen for unconfined aquifers.

3.2. GRACE Derived GWS

In Figure 4a, the black line shows ΔTWS estimated from GRACE data after leakage correction via the CLD method. Annual peaks are observed during winter mainly due to the annual cycle of precipitation. The green line shows variations of surface water (ΔSW), derived from the WaterGAP model data, and the orange line shows variations of SM (ΔSM), from ESA CCI SM and the EF. The annual amplitude of ΔSM is much larger than ΔSW, implying a greater contribution to ΔTWS and its importance in understanding ΔGWS with ΔTWS. The summer low and winter high are the same as other terms because of the precipitation change. Estimated ΔGWS obtained from ΔTWS − ΔSW − ΔSM, the blue line in Figure 4a, exhibits similar variations to the groundwater level change in the unconfined aquifer (red line in Figure 3). This finding aligns well with the previous study conducted for the entire Victoria region (Chen et al., 2016).

We validate our ΔGWS data by comparing them with in situ groundwater level data shown in Figure 3. To convert groundwater level data to groundwater storage in mass (kg/m^2), the S_y and S_sb values obtained from Equations 8 and 10 were used. Estimated S_y and S_sb and their uncertainties with 95% confidence intervals are 0.095 ± 0.022 and -0.003 ± 0.023, respectively. Both S_y and S_sb showed reasonable values, with groundwater changes primarily influenced by the unconfined aquifer. Since there are no data available for S_y in this region, we compared it with the Murray-Darling Basin value (~0.1) (Leblanc et al., 2009) near the study area. Our value for S_y (=0.095) is similar, giving us confidence in the ΔGWS estimate for southern Victoria. A minor difference would be expected for different regions (southern Victoria) versus the entire Murray-Darling Basin. Due to the coarse spatial resolution of GRACE data, this study is limited estimating aquifer parameters averaged over the entire study region. Estimations of S_y and S_sb at six sub-basins shown in Figure 1 would be plausible with finer spatial scale TWS change estimated with a revised CLD incorporating in situ SM data (Kim et al., 2025).

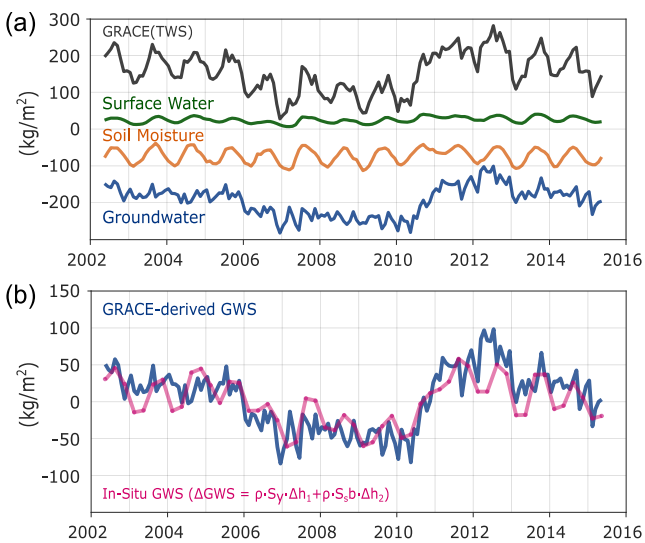

Figure 4. (a) Time series change of total water storage (ΔTWS), surface water (ΔSW), soil moisture (ΔSM), and estimated groundwater storage change (ΔGWS). Vertical offsets were added to the lines to enhance the clarity of comparisons. (b) ΔGWS estimated from ΔTWS − ΔSW − ΔSM and groundwater level multiplied by S_y (estimated from Equation 8) and ρ.

The magenta line in Figure 4b represents ΔGWS estimated from unconfined aquifer and confined aquifer level variations multiplied by S_y and S_sb respectively, and water density. While the spatial interpolation used in the groundwater data set introduces smoothing that limits the detection of high-frequency signals, the GRACE-derived results show strong consistency with the data at lower frequencies.

The ΔGWS estimate for 2002–2010, overlapping the Millennium drought, shows that groundwater storage decreased by about 100 kg/m^2 (or 10 cm equivalent water thickness), and recovered to its previous level within the period 2011–2012. After peaking in 2012, it decreased until May 2015, during the second drought period. Groundwater storage changes from in situ levels (magenta line) closely follow long-term variations in ΔGWS providing confidence in our approach to combining GRACE and ESA CCI SM. ΔGWS variations, on the other hand, differ in seasonal variations, due possibly to the influence of seasonal barometric pressure to water level of unconfined aquifer.

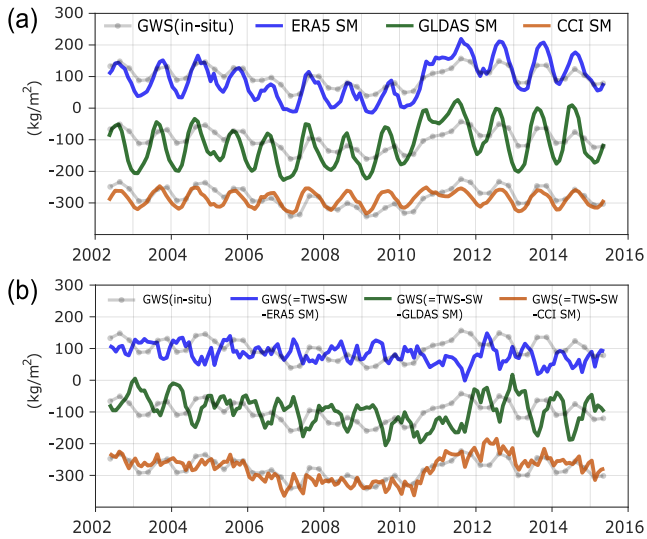

Figure 5. (a) Soil moisture and Groundwater storage (GWS) in southern Victoria. (b) GWS using Gravity Recovery and Climate Experiment terrestrial water storage and ERA5, Global Land Data Assimilation System, and European Space Agency's Climate Change Initiative for Soil Moisture. Vertical offsets were added to the lines to enhance the clarity of comparisons.

3.3. Comparison With GWS Estimates Using Model Soil Moisture Data

Many previous studies of groundwater variations with GRACE ΔTWS employed SM estimates from LSM (e.g., Strassberg et al. (2007), Rodell et al. (2009), Leblanc et al. (2009), Famiglietti et al. (2011), Munier et al. (2012), Shamsudduha et al. (2012), Chen et al. (2016), Khaki et al. (2018), Li et al. (2019) and Ali et al. (2021)). GLDAS and ERA5 have been commonly used for this purpose. However, these models have difficulty distinguishing between unsaturated and saturated zones, potentially leading to overestimations of SM and subsequent errors in groundwater storage estimates. Figure 5a shows ΔGWS (gray) derived from in situ data and ΔSM from ESA CCI and EF (orange), GLDAS (green), and ERA5 (blue). The gray lines are identical but placed separately to compare with each ΔSM. Long-term variations in both GLDAS and ERA5 ΔSM closely agree with those in groundwater storage, indicating LSM ΔSM would include groundwater contributions. Figure 5b shows ΔGWS variations obtained using GRACE ΔTWS and various ΔSM from ERA5 (blue), GLDAS (green), and ESA CCI incorporating EF (orange), respectively. It aligns best with in situ derived ΔGWS (gray) when ESA CCI SM is used. The scatter plots and the R-squared values for each case are provided in Supporting Information S1 (Figure S5).

3.4. Comparing Results Using GRACE Mascons

In this study, GRACE ΔTWS was estimated via the CLD method to suppress spatial leakage. Mascon solutions (Save, 2020; Save et al., 2016) are nominally free of such leakage. ΔTWS from Mascon and CLD (Figure 6a) appear similar but in situ groundwater level changes reveal significant differences. Applying the same approach to the Mascon solution ΔTWS, estimated S_y and $S_s b$ and uncertainties with 95% confidence intervals were 0.052 ± 0.019 and -0.019 ± 0.021, respectively. In this case, $S_s b$ is negative but not significantly so. Furthermore, the estimated S_y (0.052 ± 0.019) is about half the previous in situ estimate (Leblanc et al., 2009). The estimated ΔGWS based on Mascon ΔTWS (green line in Figure 6b) shows different annual variations with reduced inter-annual variability relative to ΔGWS using CLD to estimate TWS (black line in Figure 6b). This shows the importance of inter-basin leakage correction in GWS studies with GRACE TWS.

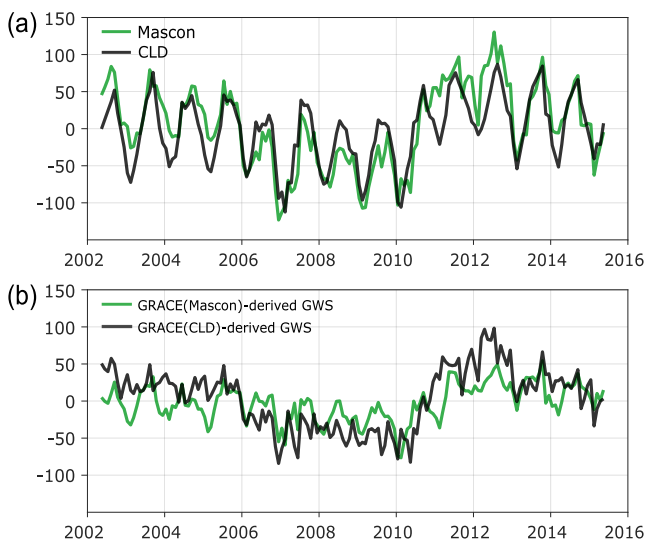

Figure 6. (a) ΔTWS provided by Mascon solutions (green) and constrained linear deconvolution (CLD) (black). (b) ΔGWS estimated from Mascon solution (green) and CLD (black) ΔTWS after correction of ΔSW and ΔSM.

4. Summary and Conclusions

GRACE is a valuable space-based observational platform for estimating groundwater storage changes (ΔGWS) providing other terrestrial water storage (ΔTWS) sources are accounted for, in particular SM (ΔSM). ΔSM from LSM has been widely employed for this purpose without robust validation. Uncertainties in LSM likely limited the quality of ΔGWS variations in previous studies. Here, SM for the top 2 cm layer is taken from observations (ESA CCI), with extrapolation to root zone depth via an EF. The original EF approach by Albergel et al. (2008) is based on a one-layer estimation. As pointed out in recent studies by Sehgal et al. (2024) and Ouaadi et al. (2025), the EF parameter may vary considerably depending on soil characteristics. To address this, the present study applies a multi-layer EF method to account for depth-dependent variations in soil properties. The comparison between SM estimated using the revised EF method and observations from in situ stations confirms the robustness of the multi-layer EF method (Figures S2 in Supporting Information S1). The estimated ΔSM differs notably from those of LSM.

Our method of ΔGWS estimation, which depends solely on the observed ΔTWS and ΔSM from space, was tested in the southern Victoria region of Australia where extensive in situ groundwater monitoring data is available.

Our method showed clear improvement of ΔGWS estimates in reproducing both seasonal and interannual variability of in situ GWS over the analysis period when compared with conventional estimates from ERA5 and GLDAS SM. Particularly, GWS recovery from the end of the Millennium Drought, 2010, was found only in the estimate from CCI SM. In addition, comparison of Δ GWS from GRACE and in situ measurements enabled estimation of mean storage coefficients in the study region. The estimated S_y for unconfined aquifers and $S_s b$ for confined aquifer were 0.095 ± 0.022 and -0.003 ± 0.023, respectively. Close alignment of the estimated storage coefficients with in situ observations supports the robustness of our estimated GWS variations.

Anomalous variations of ΔGWS and ΔSM forced by climate warming were reported in many regions. In particular, as warming persists, continuous groundwater depletion is expected and the connection between ΔSM and ΔGWS would be altered. This study would be potentially useful to understand such changes in hydrological response to a warming climate in major aquifers. Recent studies report long-term decline of TWS, mainly in SM (Seo et al., 2025) and groundwater (Seo et al., 2023). Long-term decline of TWS poses serious risks in sustainable water management and demands timely development of adaptation strategies guided by regional to global scale water resources monitoring. However, current LSM show limited capability of reproducing long-term trends of TWS, particularly changes in groundwater (Forootan et al., 2024). The method developed in this study can make important contributions to improve current practices of groundwater accounting and management policies, which have so far relied on sparse monitoring wells and simple hydrological models. This is particularly important for heavily managed large basins, such as the Colorado River Basin of the US and the Murray Darling Basin of Australia where non-natural redistribution and lateral transport of water exerts strong influence on sub-basin-scale water balance.

Lastly, continuing studies on improving spatial resolution of GRACE observations (e.g. (Kim et al., 2024; Kim et al., 2025),) and longer monitoring records in coming years will eventually broaden their applicability to smaller catchments and enable more robust climatological assessment of the groundwater storage from GRACE.

Conflict of Interest

The authors declare no conflicts of interest relevant to this study.

Data Availability Statement

The GRACE CLD data used in this study are available at (Kim et al., 2024). WaterGap data can be downloaded at (Schmied et al., 2021). ESA CCI SM data can be downloaded at (Dorigo et al., 2023). Root zone depth data can be downloaded at (Schenk & Jackson, 2009). ERA5 SM data can be downloaded at (Muñoz Sabater, 2019). GLDAS SM data can be downloaded at (Beaudoing & Rodell, 2020). CSR mascon data is available at (Save, 2020). The result data for this study are available at http://geodesy.snu.ac.kr/bbs/board.php?bo_table=sub5_1&wr_id=19.

Acknowledgments
This study was supported by the Korea Institute of Marine Science & Technology Promotion (KIMST) funded by the Ministry of Ocean Fisheries, Korea (RS-2023-00256677; PM25020), National Research Foundation of Korea (NRF) Grant (RS-2023-NR076591), the BK21 FOUR Program through the Center for Science Education in the Infosphere. J. K. is supported by NRF (RS-2024-00346384). JC was supported by the NSFC Major Programme (42394132) and Hong Kong RGC Collaborative Research Fund (C5013-23G), and CRW is supported by NASA GRACE-FO Grant 80NSSC20K0820 and ESI Grant 80NSSC22K0906.

References

Albergel, C., Rüdiger, C., Pellarin, T., Calvet, J. C., Fritz, N., Froissard, F., et al. (2008). From near-surface to root-zone soil moisture using an exponential filter: An assessment of the method based on in-situ observations and model simulations. *Hydrology and Earth System Sciences*, *12*(6), 1323–1337. https://doi.org/10.5194/hess-12-1323-2008

Ali, S., Liu, D., Fu, Q., Cheema, M. J. M., Pham, Q. B., Rahaman, M. M., et al. (2021). Improving the resolution of GRACE data for spatio-temporal groundwater storage assessment. *Remote Sensing*, *13*(17), 3513. https://doi.org/10.3390/rs13173513

Ashraf, S., Nazemi, A., & AghaKouchak, A. (2021). Anthropogenic drought dominates groundwater depletion in Iran. *Scientific Reports*, *11*(1), 9135. https://doi.org/10.1038/s41598-021-88522-y

Batu, V. (1998). *Aquifer hydraulics: A comprehensive guide to hydrogeologic data analysis*. Wiley. Retrieved from https://books.google.co.kr/books?id=JncPuWYf5qMC

Beaudoing, H., & Rodell, M. (2020). GLDAS Noah land surface model L4 monthly 0.25 x 0.25 degree V2.1 [Dataset]. https://doi.org/10.5067/SXAVCZFAQLNO

Castellazzi, P., Ransley, T., Mcpherson, A., Slatter, E., Frost, A., Shokri, A., et al. (2024). Assessing groundwater storage change in the great artesian basin using GRACE and groundwater budgets. *Water Resources Research*, *60*(11), e2024WR037334. https://doi.org/10.1029/2024WR037334

Chen, J. L., Wilson, C. R., Tapley, B. D., Scanlon, B., & Güntner, A. (2016). Long-term groundwater storage change in Victoria, Australia from satellite gravity and observations. *Global and Planetary Change*, *139*, 56–65. https://doi.org/10.1016/j.gloplacha.2016.01.002

Condon, L. E., Kollet, S., Bierkens, M. F. P., Fogg, G. E., Maxwell, R. M., Hill, M. C., et al. (2021). Global groundwater modeling and monitoring: Opportunities and challenges. *Water Resources Research*, *57*(12), e2020WR029500. https://doi.org/10.1029/2020WR029500

Dangar, S., Asoka, A., & Mishra, V. (2021). Causes and implications of groundwater depletion in India: A review. *Journal of Hydrology*, *596*, 126103. https://doi.org/10.1016/j.jhydrol.2021.126103

Dorigo, W., Preimesberger, W., Hahn, S., Van der Schalie, R., De Jeu, R., Kidd, R., et al. (2023). ESA soil moisture climate change initiative (Soil_Moisture_cci): Version 08.1 data collection [Dataset]. Retrieved from http://catalogue.ceda.ac.uk/uuid/ff890589c21f4033803aa550f52c980c/

Famiglietti, J. S., Lo, M., Ho, S. L., Bethune, J., Anderson, K. J., Syed, T. H., et al. (2011). Satellites measure recent rates of groundwater depletion in California's central valley. *Geophysical Research Letters*, *38*(3), L03403. https://doi.org/10.1029/2010gl046442

Feng, W., Shum, C. K., Zhong, M., & Pan, Y. (2018). Groundwater storage changes in China from satellite gravity: An overview. *Remote Sensing*, *10*(5), 674. https://doi.org/10.3390/rs10050674

Forootan, E., Mehrnegar, N., Schumacher, M., Schiettekatte, L. A. R., Jagdhuber, T., Farzaneh, S., et al. (2024). Global groundwater droughts are more severe than they appear in hydrological models: An investigation through a Bayesian merging of GRACE and GRACE-FO data with a water balance model. *Science of the Total Environment*, *912*, 169476. https://doi.org/10.1016/j.scitotenv.2023.169476

Fowler, K., Knoben, W. J. M., Peel, M. C., Peterson, T. J., Ryu, D., Saft, M., et al. (2020). Many commonly used rainfall-runoff models lack long, slow dynamics: Implications for runoff projections. *Water Resources Research*, *56*(5), e2019WR025286. https://doi.org/10.1029/2019WR025286

Frappart, F., & Ramillien, G. (2018). Monitoring groundwater storage changes using the gravity recovery and climate experiment (GRACE) satellite mission: A review. *Remote Sensing*, *10*(6), 829. https://doi.org/10.3390/rs10060829

GHD. (2012). Victorian aquifer framework updates for seamless mapping of aquifer surfaces. Retrieved from https://www.vvg.org.au/cb_pages/files/207086.pdf

Gleeson, T., Wada, Y., Bierkens, M. F. P., & van Beek, L. P. H. (2012). Water balance of global aquifers revealed by groundwater footprint. *Nature*, *488*(7410), 197–200. https://doi.org/10.1038/nature11295

Jasechko, S., Seybold, H., Perrone, D., Fan, Y., Shamsudduha, M., Taylor, R. G., et al. (2024). Rapid groundwater decline and some cases of recovery in aquifers globally. *Nature*, *625*(7996), 715–721. https://doi.org/10.1038/s41586-023-06879-8

Khaki, M., Forootan, E., Kuhn, M., Awange, J., van Dijk, A. I. J. M., Schumacher, M., & Sharifie, M. A. (2018). Determining water storage depletion within Iran by assimilating GRACE data into the W3RA hydrological model. *Advances in Water Resources*, *114*, 1–18. https://doi.org/10.1016/j.advwatres.2018.02.008

Kim, J., Ryu, D., Seo, K.-W., & Fowler, K. (2025). Downscaling GRACE-FO data with CYGNSS soil moisture for improved representation of floodplain inundation: Application to the murray-darling basin, Australia. *EGU General Assembly*. Vienna, Austria. https://doi.org/10.5194/egusphere-egu25-7840

Kim, J. S., Seo, K. W., Kim, B. H., Ryu, D., Chen, J. L., & Wilson, C. (2024). High-resolution terrestrial water storage estimates from GRACE and land surface models. *Water Resources Research*, *60*(2), e2023WR035483. https://doi.org/10.1029/2023WR035483

Konikow, L. F. (2015). Long-term groundwater depletion in the United States. *Groundwater Series*, *53*(1), 2–9. https://doi.org/10.1111/gwat.12306

Leblanc, M. J., Tregoning, P., Ramillien, G., Tweed, S. O., & Fakes, A. (2009). Basin-scale, integrated observations of the early 21st century multiyear drought in southeast Australia. *Water Resources Research*, *45*(4), W04408. https://doi.org/10.1029/2008wr007333

Li, B. L., Rodell, M., Kumar, S., Beaudoing, H. K., Getirana, A., Zaitchik, B. F., et al. (2019). Global GRACE data assimilation for groundwater and drought monitoring: Advances and challenges. *Water Resources Research*, *55*(9), 7564–7586. https://doi.org/10.1029/2018wr024618

Menke, W. (2012). *Geophysical data analysis: Discrete inverse theory: MATLAB edition*. Elsevier Science. Retrieved from https://books.google.co.kr/books?id=RHAdIJrUXukC

Munier, S., Becker, M., Maisongrande, P., & Cazenave, A. (2012). Using GRACE to detect groundwater storage variations: The cases of canning basin and Guarani aquifer system. *International Water Technology Journal*, *2*, 2–13. https://hal.science/hal-01162472

Muñoz Sabater, J. (2019). ERA5-Land hourly data from 1950 to present [Dataset]. https://doi.org/10.24381/cds.e2161bac

Ouaadi, N., Chehbouni, A., Ayari, E., Hssaine, B. A., ElFarkh, J., Le Page, M., et al. (2025). Root zone soil moisture mapping at very high spatial resolution using radar-derived surface soil moisture product. *Agricultural Water Management*, *314*, 109507. https://doi.org/10.1016/j.agwat.2025.109507

Pasik, A., Gruber, A., Preimesberger, W., De Santis, D., & Dorigo, W. (2023). Uncertainty estimation for a new exponential-filter-based long-term root-zone soil moisture dataset from copernicus climate change service (C3S) surface observations. *Geoscientific Model Development*, *16*(17), 4957–4976. https://doi.org/10.5194/gmd-16-4957-2023

Peterson, T. J., Saft, M., Peel, M., & John, A. (2021). Watersheds may not recover from drought. *Science*, *372*(6543), 745–749. https://doi.org/10.1126/science.abd5085

Rodell, M., Velicogna, I., & Famiglietti, J. S. (2009). Satellite-based estimates of groundwater depletion in India. *Nature*, *460*(7258), 999–1002. https://doi.org/10.1038/nature08238

Save, H. (2020). CSR GRACE and GRACE-FO RL06 mascon solutions v02 [Dataset]. https://doi.org/10.15781/cgq9-nh24

Save, H., Bettadpur, S., & Tapley, B. D. (2016). High-resolution CSR GRACE RL05 mascons [Dataset]. *Journal of Geophysical Research-Solid Earth*, *121*(10), 7547–7569. https://doi.org/10.1002/2016jb013007

Schenk, H. J., & Jackson, R. B. (2009). ISLSCP II ecosystem rooting depths [Dataset]. *ORNL Distributed Active Archive Center Datasets*. https://doi.org/10.3334/ORNLDAAC/929

Schmied, H. M., Cáceres, D., Eisner, S., Flörke, M., Herbert, C., Niemann, C., et al. (2021). The global water resources and use model WaterGAP v2.2d: Model description and evaluation [Dataset]. *Geoscientific Model Development*, *14*(2), 1037–1079. https://doi.org/10.5194/gmd-14-1037-2021

Sehgal, V., Mohanty, B. P., & Reichle, R. H. (2024). Rootzone soil moisture dynamics using terrestrial water-energy coupling. *Geophysical Research Letters*, *51*(19), e2024GL110342. https://doi.org/10.1029/2024GL110342

Seo, K. W., Ryu, D., Eom, J., Jeon, T., Kim, J. S., Youm, K., et al. (2023). Drift of Earth's pole confirms groundwater depletion as a significant contributor to global sea level rise 1993-2010. *Geophysical Research Letters*, *50*(12), e2023GL103509. https://doi.org/10.1029/2023GL103509

Seo, K. W., Ryu, D., Jeon, T., Youm, K., Kim, J. S., Oh, E. H., et al. (2025). Abrupt sea level rise and Earth's gradual pole shift reveal permanent hydrological regime changes in the 21st century. *Science*, *387*(6741), 1408–1413. https://doi.org/10.1126/science.adq6529

Shamsudduha, M., Taylor, R. G., & Longuevergne, L. (2012). Monitoring groundwater storage changes in the highly seasonal humid tropics: Validation of GRACE measurements in the Bengal Basin. *Water Resources Research*, *48*(2), W02508. https://doi.org/10.1029/2011wr010993

Smith, M., Cross, K., Paden, M., & Laban, P. (2016). Spring – Managing groundwater sustainably. https://doi.org/10.2305/IUCN.CH.2016.WANI.8.en

Strassberg, G., Scanlon, B. R., & Rodell, M. (2007). Comparison of seasonal terrestrial water storage variations from GRACE with groundwater-level measurements from the high plains aquifer (USA). *Geophysical Research Letters*, *34*(14), L14402. https://doi.org/10.1029/2007gl030139

Stroud, P. D. (1999). A recursive exponential filter for time-sensitive data. *Los Alamos National Laboratory, Tech. Rep. LAUR-99-5573*, 131. https://api.semanticscholar.org/CorpusID:16412279

Tapley, B. D., Watkins, M. M., Flechtner, F., Reigber, C., Bettadpur, S., Rodell, M., et al. (2019). Contributions of GRACE to understanding climate change. *Nature Climate Change*, *9*(5), 358–369. https://doi.org/10.1038/s41558-019-0456-2

Tromp-van Meerveld, H. J., & McDonnell, J. J. (2006). On the interrelations between topography, soil depth, soil moisture, transpiration rates and species distribution at the hillslope scale. *Advances in Water Resources*, *29*(2), 293–310. https://doi.org/10.1016/j.advwatres.2005.02.016

Wagner, W., Lemoine, G., & Rott, H. (1999). A method for estimating soil moisture from ERS scatterometer and soil data. *Remote Sensing of Environment*, *70*(2), 191–207. https://doi.org/10.1016/S0034-4257(99)00036-X

Weligamage, H. G., Fowler, K., Peterson, T. J., Saft, M., Peel, M. C., & Ryu, D. (2023). Partitioning of precipitation into terrestrial water balance components under a drying climate. *Water Resources Research*, *59*(5), e2022WR033538. https://doi.org/10.1029/2022WR033538